Kuwait J.Sci., Vol.48, No.(4),October.2021,pp(1-11)

A new intelligent time series prediction technique for coherency identification performance enhancement

Ainnur F. I. M. Shah[1], Mohd A. M. Ariff [2,*], Nadhirah Omar[3], Muhammad S. A. Mustaza[4]
Faculty of Electrical and Electronics Engineering
University Tun Hussein Onn Malaysia, 86400 Batu Pahat, Johor, Malaysia
**Corresponding author: aifaa@uthm.edu.my*

Abstract

The manuscript proposes a time series prediction technique to enhance the response time of the coherency identification technique. The proposed methodology utilizes the nonlinear autoregressive exogenous neural network (NARX) algorithm to predict the generator speed deviations following a disturbance in the system. Consequently, the coherency identification technique based on independent component analysis (ICA) is utilized on the predicted system responses. The effectiveness of the proposed approach is demonstrated on of the IEEE 16-generator 68-bus test system model. The result shows that the proposed technique can predict 0.2s following a disturbance in the system accurately. Therefore, the NARX allows a 0.2s head start for the ICA to determine the real-time coherent generator group in the system. Furthermore, the result shows that the proposed approach can identify the coherent group of generators based on the predicted generator speed deviation in all cases considered in this study, accurately. Conclusively, the result implies that the proposed technique can speed up the overall coherency identification process in a power system operation.

Keywords: Artificial neural network; coherency identification; nonlinear autoregressive exogenous; power system; time series prediction.

1. Introduction

The modernization of power systems has brought a revolution in the electricity generation and distribution sectors in recent years Koochi *et al.,* (2019), Biyik & Husein, (2018). In a smart grid operating environment, the stochastic nature of renewable energy sources have been a challenge in managing the stable energy supply. The challenge is mainly due to the fact that the electricity generated from the renewable resources are not to control to fulfill to the variation of the consumer's demand Talari *et al.,* (2018). Consequently, the inclusion of sustainable energy storage systems increase the difficulties for system operators to come out with effective measures to control the network in the presence of a disturbance Ak *et al.,* (2015). Therefore, the power system network needs to be simplified to ease the decision-making process when necessary. One well-accepted solution to simplify the network is by identifying the coherent groups of generators that have a similar dynamic response Chow, (2013).

Coherency identification has been utilized to minimize the power system control effort by locating the weak link between the coherent areas Rezaeian *et al.,* (2017). Thus, the coherency identification technique allows the operator to focus on the reinforcement of the weak link to improve the power system stability. The technique has evolved throughout the year Lin *et al.,* (2017). It can be determined by using coherency identification based on the model or measurement method. In the measurement-based process, the rotor angles, generator speed and voltage magnitudes reflect the dynamic response of generator Khalil & Iravani, (2015). Based on these measures, the coherent generator groups are formed by identifying the closely coupled generators in inter-area modes Wei *et al.,* (2019).

In a smart grid operating environment, these groups of generators are varying with time, especially with the integration of the stochastic renewable energy resources Nayak & Nayak, (2018). Thus, it is crucial to identify the real-time coherency group of the generator to provide an accurate control measures following a disturbance in the system. Identifying the real-time coherency group can be a challenging task as the system is represented by thousands of differential-algebraic practice equation. Although the coherency identification method discussed in the literature can identify the group in near real-time, the reported performance does not allocate ample time for the system operator to process and provide the required control action. Thus, this challenge motivates the power system researchers and engineers to predict the time series of the system dynamic behavior to give an analytical tool, such as the coherency identification method, a head start to analyze and decide onpredicted signal. The time series prediction has been utilized in various data-driven methods in power system applications Ma & Vittal, (2012).

This work presented in this paper aims to predict the time series of the generator dynamic response for the measurement-based coherency identification application. The time series prediction an algorithm is based on NARX to predict the generator speed deviation following a disturbance in the system. Consequently, the predicted generator speed deviation is applied to a data-driven coherency identification technique based on the independent component analysis (ICA) Ariff & Pal, (2012). The proposed NARX time series predictor is expected to enhance the overall performance of the coherency identification process using ICA. The proposed method is simple and does not require any prior system information during operation.

2. State of the art

In the light of smart grid development, the exploration of the time series prediction in power system application has gained more attention to fulfill the demand for fast and instantaneous control action. A time series prediction method based on Boltzmann algorithm is reported in Zhang *et al.,* (2015) to predict the wind speed of an area to assist the wind farm operation. The algorithm is a variant of recurrent neural network (RNN), which has demonstrated its performance in handling nonlinear data. However, its performancein predicting the wind speed is highly dependent on the optimal deep model selection and its suitability varies with the application. In Liu *et al.,* (2015), a support vector machine (SVM) is utilized to predict the failure of the reactor coolant pump component in a typical nuclear-pressurized water reactor. The method combines the SVM method with radial basis function (RBF) to predict the time series behavior of the reactor components. It can predict the response of the component one day ahead of its time. However, the reported SVM method requires an additional tuning process of hyperparameters to achieve the desired performance. Next, the researchers in Nazaripouya *et al.,* (2016) predict the solar power output of a PV based on the historical time series data. The method is based on the combination of wavelet analysis, auto-regressive moving average (ARMA) and RNN to predict one-minute solar power output. From the discussion, the method can predict the slow dynamic events in the power system, accurately. A hybrid method is reported in Silva *et al.,* (2017) to predict the load curves of the residential and the commercial customers. In this report, the combination of seasonal autoregressive fractionally integrated moving average (SARFIMA) and fuzzy time series (FTS) method. In this paper, the load curves are viewed as a long memory time series. As a result, the method requires fewer input parameters to estimate the future time series accurately. The researchers in Wang *et al.,* (2018) report a methodology to predict wind power using the distance weighted kernel density estimation. The method is used to capture the stochastic behavior of the non-stationary wind power time series. Despite the effectiveness of the method, it is very challenging to find a satisfactory balance between the prediction accuracy and the computational speed due to the unpredictability of the wind power. Consequently, the kernel density estimation method is combined with the fuzzy inference system and the tri-level adaptation function to capture the uncertainties of the prediction model and the wind power time series Khorramdel *et al.,* (2018). The work presented Wang, *et al.,* (2020) combines particle swarm optimization (PSO), ARMA, and SVM by using clustering theory to predict the wind power time series for large-scale of wind power integration applications. It is relatively complex as compared to other methods.

The application of this method requires additional weight optimization to acquire adequate wind power prediction precision. Moreover, Khan *et al.,* (2020), the researchers combine the multilayer perceptron (MLP), SVR, and CatBoost to predict the actual energy consumption in Jeju Island. The combination of renewable and non-renewable energy data sources is used as training data for the proposed model. However, the hybrid approach complicates the process since each technique requires the hyperparameters tuned to give the optimal model. On the other hand, a hybrid method reported in Sarica *et al.,* (2018) based on autoregressive (AR) and neuro-fuzzy inference system (ANFIS) are combined to reduce the parameters and rules of ANFIS. However, the model focuses on predicting the time series responses for a small test system only.

It is observed that the methods reviewed in the literature are dependable to predict the time series in various fields in the power system application. However, most of the reported methods are hybrid, which combines several methods to achieve the desired prediction performance. In addition, the methods reported in Nazaripouya *et al.,* (2016); Silva *et al.,* (2017); Wang, *et al.,* (2020); Khan *et al.,* (2020) require additional parameter tuning in order to obtain a satisfactory performance in estimating future time series. Thus, the computational the complexity of the methods is excessive, and it is very challenging to be implemented in practice. Consequently, a time series prediction method based on the NARX model is proposed in this paper to predict the future time series of dynamic generator response. The proposed method is simple and accurate. The application of the NARX model has been reported in Guzman *et al.,* (2017) and Liu *et al.,* (2016). The method demonstrates promising performance in predicting the future time series of a non-linear system. This is due to the fact that the NARX network has an embedded memory that facilitates an excellent time-prediction architecture to propagate the information and backpropagate the error signal Guzman *et al.,* (2017). Therefore, NARX can predict the future time series accurately without any hybridization from other methods to improve its performance. The results this paper shows that the proposed method outperforms among the other hybrid technique in term of computational complexity.

3. Development of training dataset for time series prediction

In this section, the IEEE 16-generator 68-bus test the system model is used in this analysis to simulate the system response for various system operating situations. The transmission line, bus, and dynamic features of the test system model can be found in Pal & Chaudhuri, (2006). Figure 1 represents the single-line diagram of the IEEE 16-generator 68-bus test system model. The nonlinear simulation is performed in MATLAB Simulink. In this research, the 100Hz sampling frequency is used as suggested in Martin, (2015). Historically, the test system model consists of 5 coherent areas Rogers, (2012). However, the real-time coherent areas are depended on various factors such as fault location, fault severity, and the operating situation of the generators Saha *et al.,* (2009).

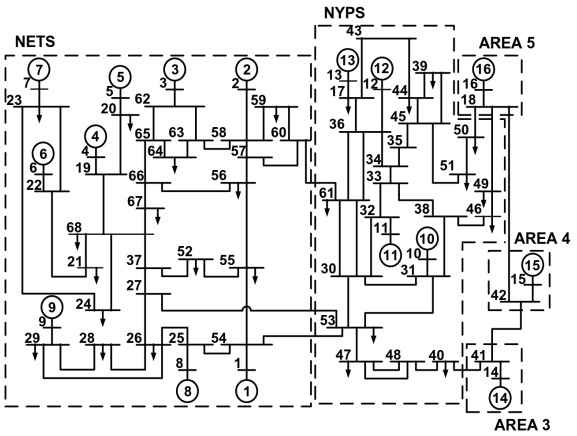

Fig. 1. Single-line diagram of the 16-generator 68-bus test system model.

In order to develop the comprehensive training dataset, the time series behavior of all generators following a disturbance is required. Then, a three-phase fault applied at every bus is considered a disturbance for the training dataset construction. In this study, only stable cases are considered. Figure 2 indicates the speed deviation for all generators for the fault at Bus 1. After 0.14s, the fault was cleared by opening the transmission line between Bus 1 and Bus 2. It is noted that the generator's the response represents only one of the many cases considered to develop the dataset. The figure shows the system is stable because the generator speed is settled to a new equilibrium point following the disturbance applied to the

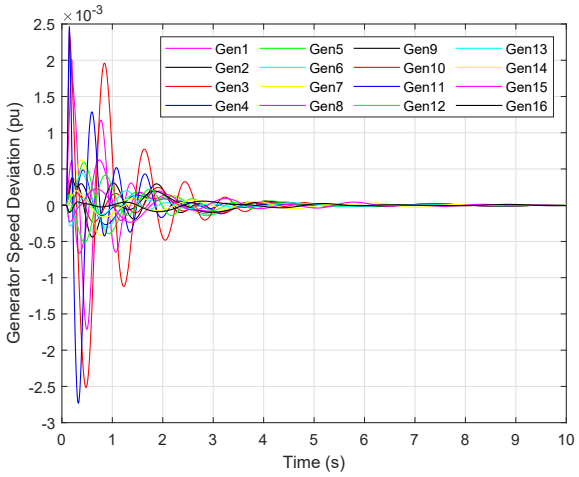

Fig. 2. Generator speed deviation on 16 generators.

system. Consequently, the input and output of the training dataset are represented as in Equation (1) and Equation (2), respectively.

$$\text{Input data, } x\left(t\right) = \omega\left(t\right), \tag{1}$$

$$\text{Output data, } y\left(t\right) = \omega\left(t + n\Delta t\right), \tag{2}$$

3.1 Development of the time series predictor

Figure 3 illustrates the NARX network utilized in this study. It is based on a parallel architecture, where the output is feedback to the input to estimate the future output. Based on that figure, the architecture consists of three layers: the input, hidden, and output layer. The input and output data are processed in the input and output layer, respectively. In this study, the generator speed deviation $\omega(t)$ is set as the input and output of the network. However, the output data is shifted by $n\Delta t$ as compared to input data. The hidden layer can be divided into two sublayers, namely as Hidden Layer 1 and Hidden Layer 2. These sublayers consist of the combination of the tapped delay line (TDL), weight, activation function, summation, and bias. The TDL introduces m-delays to the input time series and produces $\boldsymbol{m}$-dimensional vectors consist of the current input data and m-delayed data. Consequently, this matrix input data is multiplied by the interconnection weight $\mathbf{W}$ and subtracted with the bias vector $\boldsymbol{b}$. Then, the processed weighted input matrix $\mathbf{IW}$ is passed through the activation function to produce the output. These processes can be represented in Equation (3).

From equation 3,
$\mathbf{I}$ is input matrix,
$\mathbf{W}$ is weighted input matrix,
$\boldsymbol{b}$ is bias vector,
$x(t)$ is input data,
$y(t)$ is output data,
$h(t)$ is output data of Hidden Layer 1,
i is the number of neuron, and
f is the activation function.

To predict the future time series of the data, the sigmoid and linear activation functions are implemented in Hidden Layer 1 and Hidden Layer 2, respectively. These two activation functions allow the NARX network to come out with the desired decision based on the weighted input. The sigmoid and linear activation functions are represented in Equation (4) and Equation (5), accordingly. In Equation (4), s is the processed weighted input. This function permits the NARX network to adapt the non-linearity in the data by using the probability of the S-shape curve, ranging between 0 to 1. From Equation (4), the output of the Hidden Layer 1 is yielded based on the processed weighted input data classification on the S-shape curve. On the other hand, c, and l in Equation (5) represent the gradient of the linear activation function and the output data of Hidden Layer 1, respectively. This function scaled the output data of Hidden Layer 1 by c to the readjust its the magnitude to suit to the desired output data, $y\left(t\right)$. Consequently, the network weights and biases are adjusted iteratively until the error between the actual input and the target output is reduced.

$$f_1\left(s\right) = \frac{1}{1 + e^{-s}} \tag{4}$$

$$f_2\left(l\right) = cl \tag{5}$$

The selection of the network training function is critical to the prediction performance of NARX. Thus, three types of network training functions are considered and compared in this study: Levenberg-Marquardt, Bayesian Regularization, and the Scaled Conjugate Gradient. The output of the training functions is evaluated following a disturbance in the system in estimating the future time response of Generator 1 in the test

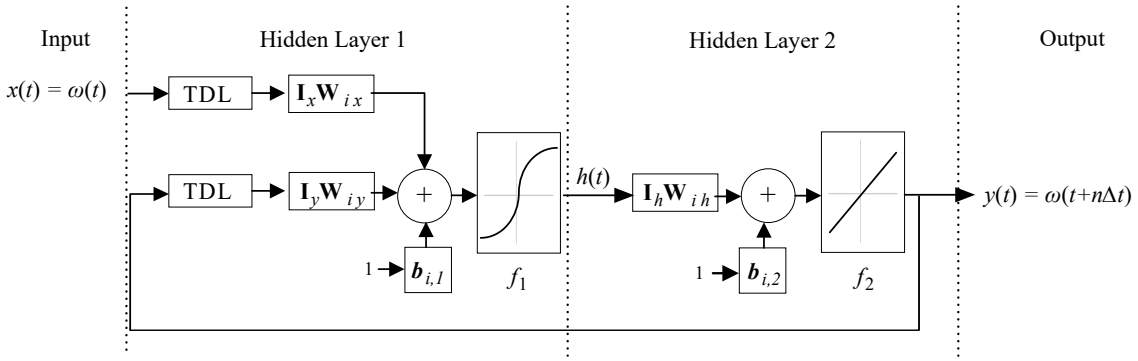

Fig. 3. Construction of NARX network utilized in this study.

$$y\left(t\right)=f_1\left(\sum_{x=1}^{n}\mathbf{I}_x\mathbf{W}_{i,x}+\sum_{y=1}^{n}\mathbf{I}_y\mathbf{W}_{i,y}+\boldsymbol{b}_{i,1}\right)+f_2\left(\sum_{h=1}^{n}\mathbf{I}_h\mathbf{W}_{i,h}+\boldsymbol{b}_{i,2}\right) \tag{3}$$

system model. The performance of the training functions is compared and analyzed based on the mean squared error (MSE) of the future time series estimation. This simple comparative study is crucial to determine which one of the network training function is the best option out of three for the power system time series prediction application. The MSE is calculated based on the difference between the actual $y\left(t\right)$ and the desired $y_{desired}\left(t\right)$ estimations as shown in Equation (6).

$$MSE=\frac{1}{n}\sum_{i=1}^{n}\left(y_{desired}\left(t\right)-y\left(t\right)\right)^2 \tag{6}$$

4. Application, analysis and discussion

4.1 Determination of training network function

Table 1 tabulates the performance of the three network training functions. From the table, the Levenberg-Marquardt technique shows a more desired result as compared to other methods. The MSE using Levenberg-Marquardt, Bayesian Regularization, and Scaled Conjugate Gradient are 4.4900×10^{-11}, 1.6592×10^{-9}, and 1.2249×10^{-7}, respectively. The result implies that the Levenberg-Marquardt technique outperforms the other two training functions. Thus, it is considered as the preferred network training function for the work presented in this paper.

Table 1. Comparison of MSE between three training network function.

Network Training Function	MSE
Levenberg-Marquardt	4.4900×10^{-11}
Bayesian Regularization	1.6592×10^{-9}
Scaled Conjugate Gradient	1.2249×10^{-7}

4.2 Determination of n-step ahead

This section aims to address the question of how many n-step in Equation (1) and Equation (2) that deliver the best prediction performance. Using the Levenberg-Marquardt technique, the NARX is trained using training databases with different variants of n-step ahead as the output. Figure 4 shows the MSE versus the n-step ahead of the training database output. From the graph, the worst MSE occurs when the $n = 10$, where the MSE is 1.45×10^{-8}. The best MSE is when $n = 20$, where the MSE is 4.49×10^{-11}. This outcome implies that the time series predictor performs best when n is set to 20 in this application. Therefore, $n = 20$ is considered to develop the training database in this study.

4.3 Future time series prediction

In the NARX training phase, the dataset is divided into three phases, where 70%, 15%, and 15% of the training dataset are utilized in the training, validation, and test phase, accordingly.

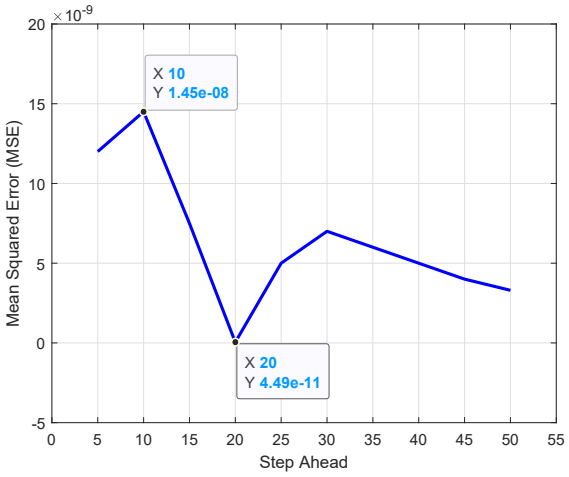

Fig. 4. MSE versus the number of a step ahead.

The performance of the training, phases depend on the regression slope R. $R = 1$ indicates that the output of the trained NARX is equal to the targeted output data. In this study, the value of R for the training, validation, and test phase are 0.99984, 0.99966, and 0.99965, respectively. Figure 5 displays the comparison between the predicted and the actual response. The solid and the dashed line represent the predicted and the actual generator responses, respectively. For better visualization of the predictor performance, only the comparison of Generator 1 is displayed and discussed here as the representative of other generators in the system. The graph shows that the time trend of the predicted outcome comes to a good agreement with the actual generator speed deviation. The results display in Figure 2 is corroborated this fact. From Figure 5, the Generator 1 speed deviation prediction starts immediately after the occurrence of the fault in the system. In practice, the implementation of the NARX predictor should be complemented with a fault detector to initiate the prediction process. From the graph, the selected peak of the predicted and the actual responses are 0.97s and 1.17s, correspondingly. The incidence of these two peaks indicates that the actual response is lagging the predicted generator response by 0.2s. The result shows that the proposed time series predictor predicts the generator speed deviation 0.2s ahead of the actual speed response. This 0.2s head start will allow ample time for various power system analytical tools such as coherency identification to assess the severity of a disturbance and provide accurate remedial control action on time. In the next subsection, the predicted generator speed deviation is applied to the measurement-based coherency identification technique based on ICA Ariff & Pal, (2012).

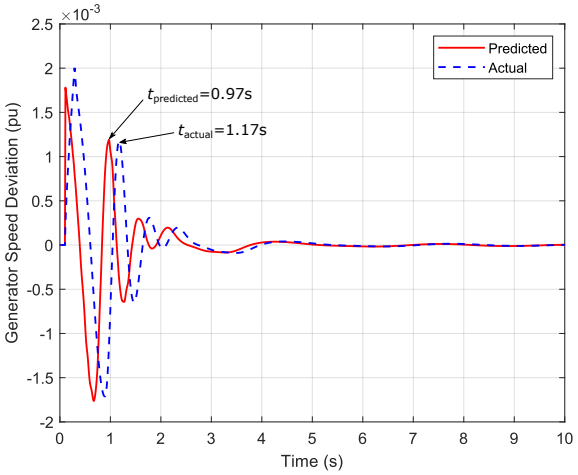

Fig. 5. The comparison of the actual and the predicted response.

4.4 Performance evaluation of time series prediction methods

This subsection evaluates the performance of MSE values in predicting the generator speed deviation for various time-step ahead. The state-of-the-art methods considered in this study are MLP Ak *et al.,* (2015), AR Pena *et al.,* (2017), SVR Liu *et al.,* (2015), AR-ANFIS Sarica *et al.,* (2018) and CatBoost-SVR-MLP Khan *et al.,* (2020). A similar dataset is used to compare the performance of all these approaches. Figure 6 displays the MSE versus the n-step ahead of the training database output. From the figure, AR shows the best accuracy based on this dataset as compared to other state-of-the-art methods. In this study, AR performs best when predicting the generator speed deviation for 15-step ahead. In contrast, SVR gives the worst MSE for $n = 35$. There are two hybrid time series prediction method considered in this study: AR-ANFIS and CatBoost-SVR-MLP. The best MSE of AR-ANFIS and CatBoost-SVR-MLP are at 2.3179×10^{-08} and 3.0008×10^{-08}, respectively. This result implies that although these methods show promising results in Sarica *et al.,* (2018) and Khan *et al.,* (2020), respectively. AR-ANFIS and CatBoost-SVR-MLP are unable

to outperform the MSE obtained using NARX. Conversely, the best MSE for NARX occurs when predicting the generator speed deviation for 20-step ahead. This performance demonstrates the proposed technique predicts the generator speed deviation 0.2s before the actual response takes place, accurately. From a power system control perspective, the control action should be taken within 0.2s following a disturbance Taylor *et al.,* (2005). This delay exists in practice due to signal delays and relay operation. Since the proposed method can predict the future time series response of the system accurately, the control mitigation algorithm such as wide-area control system (WACS) can be initiated earlier to compensate for the signal delay.

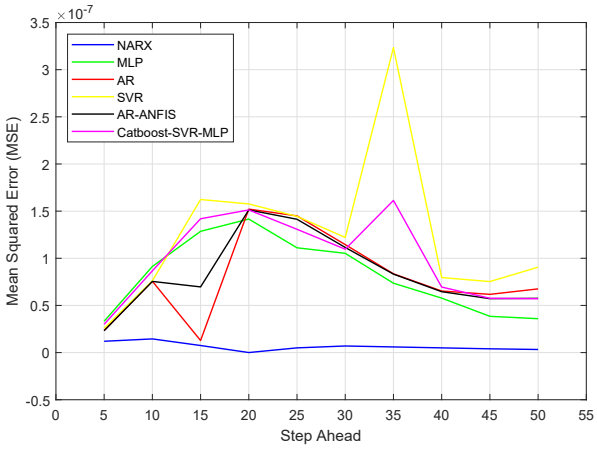

Fig. 6. MSE values achieved on 10 datasets by each time series prediction method.

4.5 Coherency identification

In this subsection, the effectiveness of the proposed the method is demonstrated on the coherency identification application in power system. The study focuses on the coherency identification in the IEEE 16-machine 68-bus test system model under two types of disturbance: a sudden increase of the generator mechanical input and a balanced three-phase fault represented as Case A and Case B, respectively. The first case is considered because it is a typical type of disturbance considered in various coherency identification studies Wei *et al.,* (2019). Conversely, a balanced three-phase fault is the most the severe disturbance that could occur in the system.

4.5.1 Case A: A sudden increase of the generator mechanical input

In this study, a 10% increment of mechanical input torque for 80ms is applied to all generators in the IEEE 16-machine 68-bus test system model. This perturbation is applied to provide the required oscillation to capture the slow coherent dynamics Cuicui *et al.,* (2019). The generator speed deviation is recorded and applied to the proposed method. Figure 7 shows the predicted generator speed deviation when the system is subjected to this disturbance. It is noted that the response shown in the figure is the 0.2s future response prediction made by the proposed NARX predictor. Then, the predicted generator speed deviation is applied to the coherency identification based on ICA. The coherency plot of the system response following this disturbance is illustrated in Figure 8.

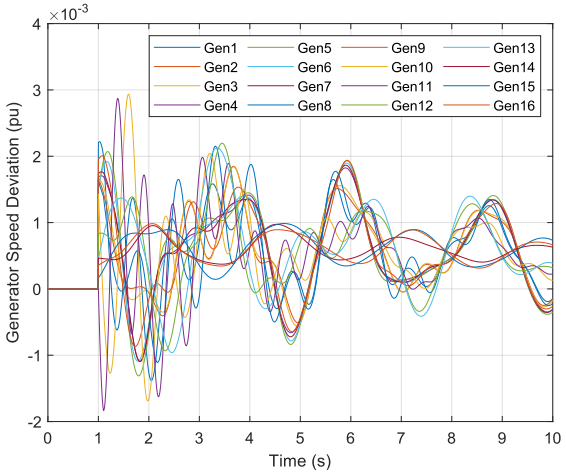

Fig. 7. Generator speed deviations for Case A.

In Figure 8, the group of coordinates in the three-dimensional coherency plot represents coherent groups of generators. It is shown that the first nine plots, G1 until G9, are relatively close to each other as compared to other generators. Thus, this group of generators is clustered as the first coherency the group is named Group 1. A similar observation can be made for G10 to G13 as these generators are well isolated from other generators as well. Thus, since G10 to G13 has a relatively similar coordinate in the three-dimensional plot, they form a different coherent group named Group 2. The other three generators, G14, G15, and G16 are separated from each other and the first two coherent groups. Thus, these generators form three separate

coherent groups named Group 3, Group 4, and Group 5, respectively. It is noted that the result obtained in this study is similar to the one reported in Ariff & Pal, (2012). This result implies that the predicted generator speed deviation using the time series NARX predictor can be implemented for the coherency identification in the system accurately.

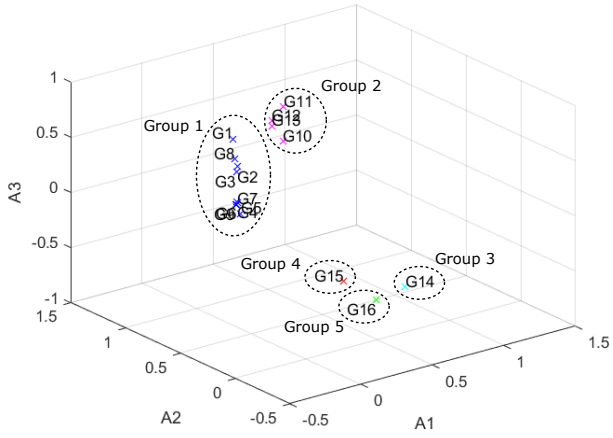

Fig. 8. Generator's coherent groups for Case A using ICA.

4.5.2 Case B: A three-phase balanced fault

This subsection shows the application of the proposed a method in corresponds to a fault in the system. In this study, a temporary balanced fault at Bus 31 for 480ms is applied to the test system model. Similar to Case A, the generator speed deviation is recorded and applied to the proposed time series predictor. Figure 9 depicts the predicted generator speed deviation for this operating situation. The NARX network predicts the generator speed deviation 0.2s ahead of the actual response. Consequently, the predicted response is applied to the ICA method to classify the coherency group of generators Ariff & Pal, (2012).

Figure 10 shows the three-dimensional coherency plot that represents this case. It is noted from Figure 9 that the generators are segregated into three coherent groups. The first group consists of G1 until G9 together with G12 until G16, namely as Group 1. These generators shared a relatively similar coordinate in the three-dimensional coherency plot and create a coherent group of generators. The second (Group

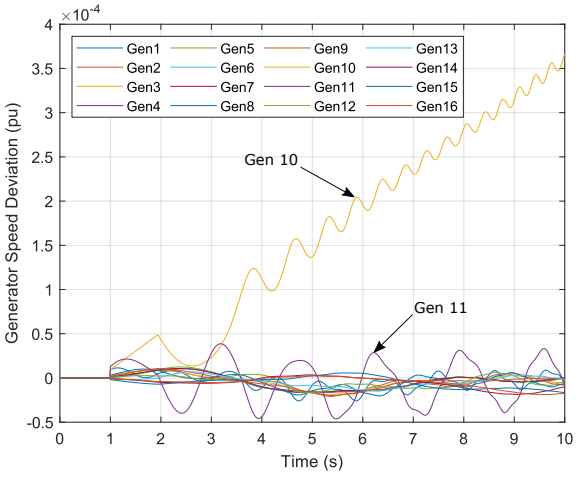

Fig. 9. Generator speed deviations for Case B.

2) and the third group (Group 3) only consist of a single generator in each group, G10, and G11, respectively. The segregation of the coherent group can also be observed from the predicted generator speed deviation responses as shown in Figure 9. In the figure, G10 oscillates away from the rest of the group, while G11 has a relatively higher oscillation as compared to other generators (generators in Group 1). This observation corroborated the segregation of the coherent group illustrated in Figure 9. The formation of this coherent group is also because the location of the fault is close to G10 and G11. Therefore, these two generators have a high tendency to oscillate against the rest of the group of generators.

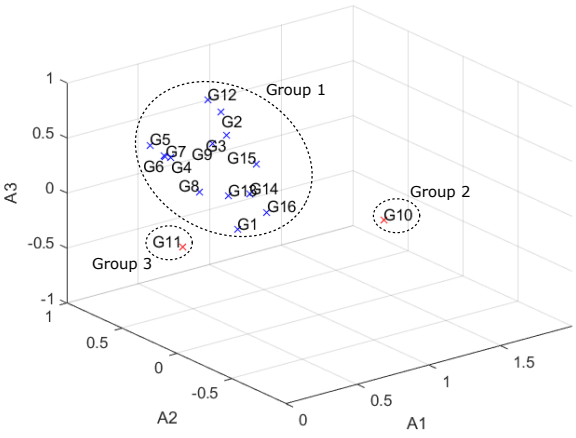

Fig. 10. Generator's coherent groups for Case B using ICA.

The most critical discussion of the results obtained from these two cases is the coherency group of generators is identified 0.2s earlier as compared to the ICA method presented in Ariff & Pal, (2012). This improvement is realized by using the proposed time series predictor based on NARX, which can provide an accurate time series prediction of the generator speed deviation 0.2s ahead of the actual event. Thus, the coherency identification method can start its algorithm 0.2s earlier. The results show that the predicted responses are accurate and can be used to identify coherent groups of generators accurately. Consequently, this implies that the proposed time series predictor based on NARX can enhance the performance of the coherency identification method using ICA. Also, the application of the predicted responses can easily be extended to any research field in power systems that utilized generator speed deviation in their algorithm such as state estimation Rinaldi *et al.,* (2018) and direct stability assessment Papadopoulos & Milanović, (2016).

5. Conclusions

Conclusively, a new time series prediction method to predict the generator speed deviation following a disturbance has been reported. The method is based on the NARX network to predict future time series ahead of the actual event. First, the generator speed deviations to form a comprehensive training dataset to train the NARX network has been performed. Consequently, the performance of various network training functions to select the best option for the time series prediction application has been conducted. Then, the prediction MSE for various n-step ahead to determine the best value of n has been determined. It is found that the NARX network performed best in estimating the generator speed deviations 0.2s ahead of its time. Also, the performance of the trained NARX network to estimate the generator speed deviations following a disturbance has been explained. The prediction of the generator speed deviation 0.2s before it happened has been discussed. The effectiveness of the proposed method based on NARX has been demonstrated to enhance the performance of coherency identification in the power system using ICA.

The application of the proposed methodology can be extended to predict various other measurements such as rotor angle, frequency, voltages and currents in the system. The predicted measurement can be applied to other research fields in the power system such as state estimation, protection and control, and stability enhancement application.

ACKNOWLEDGEMENTS

The authors would like to thank Universiti Tun Hussein Onn Malaysia (UTHM), Johor and Ministry of Higher Education (MOHE), Malaysia for awarding the grant which made this research allowed under the grant No. H406.

References

Ak, R., Fink, O., & Zio, E. (2015) Two machine learning approaches for short-term wind speed timeseries prediction. IEEE Transactions on Neural Networks and Learning Systems, 27(**8**):1734–1747.

Ariff, M., & Pal, B.C. (2012) Coherency identification in interconnected power system—an independent component analysis approach. IEEE Transactions on Power Systems, 28(**2**):1747–1755.

Biyik, E., & Husein, M. (2018) Damping wide-area oscillations in power systems: a model predictive control design. Turkish Journal of Electrical Engineering & Computer Sciences, 26(**1**):467–478.

Chow, J.H. (2013) Power system coherency and model reduction. Springer, **New York.**

Cuicui, J., Weidong, L., Liu, L., Ping, L. & Xian, W. (2019) A coherency identification method of active frequency response control based on support vector clustering for bulk power system. Energies, 12(**16**):3155.

Guzman, S.M., Paz, J.O. & Tagert, M.L.M. (2017) The use of NARX neural networks to forecast daily groundwater levels. Water resources management, 31(**5**):1591-1603.

Han, M., Zhang, S., Xu, M., Qiu, T. & Wang, N. (2018) Multivariate chaotic time series online prediction based on improved kernel recursive least squares algorithm. IEEE Transactions on Cybernetics, 49(**4**):1160-1172.

JanHendrik, M., Nils, B. & Martin, B. (2019) Distribution system monitoring for smart power grids with distributed generation using artificial

neural networks. International Journal of Electrical Power & Energy Systems, **113**:472–480.

Khalil, A.M. & Iravani, R. (2015) A dynamic coherency identification method based onfrequency deviation signals. IEEE Transactions on Power Systems, 31(**3**):1779–1787.

Khan, P.W., Byun, Y.C., Lee, S.J., Kang, D.H., Kang, J.Y. & Park, H.S. (2020) Machine learning-based approach to predict energy consumption of renewable and nonrenewable power sources. Energies, 13(**18**):4870.

Khorramdel, B., Chung, C., Safari, N. and Price, G. (2018) A fuzzy adaptive probabilistic wind power prediction framework using diffusion kernel density estimators. IEEE Transactions on Power Systems, 33(**6**):7109–7121.

Koochi, M.H.R., Dehghanian, P., Esmaeili, S., Dehghanian, P. & Wang, S. (2018) A synchrophasor-based decision tree approach for identification of most coherent generating units. IECON 2018-44th Annual Conference of the IEEE Industrial Electronics Society. Columbia, United States.

Koochi, M.H.R., Esmaeili, S. and Ledwich, G. (2019) Taxonomy of coherency detection and coherency-based methods for generators grouping and power system partitioning. IET Generation, Transmission & Distribution, 13(**12**):2597–2610.

Lin, Z., Wen, F., Ding, Y. & Xue, Y. (2017) Data driven coherency identification for generators based on spectral clustering. IEEE Transactions on Industrial Informatics, 14(**3**):1275–1285.

Liu, Y., Wang, X., Liu, Y. & Cui, S., (2016) Data-aware retrodiction for asynchronous harmonic measurement in a cyber-physical energy system. Sensors, 16(**8**):1316.

Liu, J., Vitelli, V., Zio, E. & Seraoui, R. (2015) A novel dynamic-weighted probabilistic support vector regression-based ensemble for prognostics of time series data. IEEE Transactions on Reliability, 64(**4**):1203–1213.

Lu, C., Zhang, J., Zhang, X. & Zhao, Y. (2018) Wide-area oscillation identification and damping control in power systems. Foundations and Trends in Electric Energy Systems, 2(**2**):133–197.

Ma, F. & Vittal, V. (2012) A hybrid dynamic equivalent using ANN-based boundary matching technique. IEEE Transactions on Power Systems, 27(**3**):1494–1502.

Martin, K.E. (2015) Synchrophasor measurements under the IEEE standard c37.118.1-2011 with amendment c37.118.1a. IEEE Transactions on Power Delivery, 30(**3**):1514–1522.

Nayak, C.K. & Nayak, M.R. (2018) Technoeconomic analysis of a grid-connected pv and battery energy storage system considering time of use pricing. Turkish Journal of Electrical Engineering & Computer Sciences, 26(**1**):318–329.

Nazaripouya, H., Wang, B., Wang, Y., Chu, P., Pota, H. & *et al.* (2016) Univariate time series prediction of solar power using a hybrid wavelet-ARMA-NARX prediction method. Proceedings of 2016 IEEE/PES Transmission and Distribution Conference and Exposition (T&D). Latin America, United States.

Ouyang, T., Huang, H., He, Y. & Tang, Z. (2020) Chaotic wind power time series prediction via switching data-driven modes. Renewable Energy, **145**:270-281.

Pal, B. & Chaudhuri, B. (2006) Robust control in power systems. Springer Science and Business Media, **USA.**

Papadopoulos, P.N. & Milanović, J.V. (2016) Probabilistic framework for transient stability assessment of power systems with high penetration of renewable generation. IEEE Transactions on Power Systems, 32(**4**):3078-3088.

Pena-Sanchez, Y. & Ringwood, J. (2017) A critical comparison of AR and ARMA models for short-term wave forecasting. Proceedings of the 12th European Wave & Tidal Energy Conference. Cork, Ireland.

Rezaeian, M.H., Esmaeili, S. & Fadaeinedjad, R. (2017) Generator coherency and network partitioning for dynamic equivalencing using subtractive clustering algorithm. IEEE Systems Journal, 12(**4**):3085–3095.

Rinaldi, G., Menon, P.P., Edwards, C. & Ferrara, A. (2018) Sliding mode based dynamic state estimation for synchronous generators in

power systems. IEEE control systems letters, 2(**4**):785-790.

Rogers, G. (2012) Power system oscillations. Springer Science and Business Media, **New York.**

Saha, M.M., Izykowski, J.J. & Rosolowski, E. (2009) Fault location on power networks. Springer Science and Business Media, **London.**

Sarica, B., Eĝrioĝlu, E. & Asikgil, B. (2018) A new hybrid method for time series forecasting: AR–ANFIS. Neural Computing and Applications, 29(**3**):749-760.

Silva, C., Guimarães, F.G., Sadaei, H.J. & Coelho, V.N. (2017) A hybrid SARFIMA-FTS model for time series prediction in smart grids. 2017 IEEE International Conference on Fuzzy Systems (FUZZ-IEEE). Naples, Italy.

Talari, S., Shafie-Khah, M., Osôrio, G.J., Aghaei, J. & Catalão, J.P. (2018) Stochastic modelling of renewable energy sources from operators' point-of-view: A survey. Renewable and Sustainable Energy Reviews, **81**:1953–1965.

Taylor, C.W., Erickson, D.C., Martin, K.E., Wilson, R.E. & Venkatasubramanian, V. (2005) WACS-wide-area stability and voltage control system: R&D and online demonstration. Proceedings of the IEEE Power Engineering Society General Meeting. Denver, USA.

Thakallapelli, A., Hossain, S.J. & Kamalasadan, S. (2018) Coherency and online signal selection based wide area control of wind integrated power grid. IEEE Transactions on Industry Applications, 54(**4**):3712–3722.

Wang, Y., Wang, D. & Tang,Y. (2020) Clustered hybrid wind power prediction model based on ARMA, PSO-SVM, and clustering methods. IEEE Access, **8**:17071–17079.

Wang, Z., Wang, W., Liu, C., Wang, B. & Feng, S. (2018) Short-term probabilistic forecasting for regional wind power using distance-weighted kernel density estimation. IET Renewable Power Generation, 12(**15**):1725-1732.

Wei, Y., Arunagirinathan, P., Arzani, A. & Venayagamoorthy, G.K. (2019) Situational awareness of coherency behavior of synchronous generators in a power system with utility-scale photovoltaics. Electric Power Systems Research, **172**:38–49.

Zhang, C.Y., Chen, C.P., Gan, M. & Chen, L. (2015) Predictive deep Boltzmann machine for multiperiod wind speed forecasting. IEEE Transactions on Sustainable Energy, 6(**4**):1416–1425.

Zhu, H. & Lu, X. (2016) The prediction of PM2.5 value based on ARMA and improved BP neural network model. Proceedings of International Conference on Intelligent Networking and Collaborative Systems (INCoS). Ostrawva, Czech Republic.

Zina, B., Octavian, C., Ahmed, R., Haritza, C. & Najiba, M.B., (2018) A nonlinear autoregressive exogenous (NARX) neural network model for the prediction of the daily direct solar radiation. Energies, 11(**3**):620.

Submitted: 15/07/2020
Revised: 26/11/2020
Accepted: 19/12/2020
DOI: 10.48129/kjs.v48i4.10383